

USE OF SATELLITE IMAGES LANDSAT 5 TM IN IDENTIFICATION OF ISLANDS OF HEAT IN THE CITY OF RECIFE -PE

Ana Mônica Correia¹, Werônica Meira de Souza², Romilson Ferreira da Silva¹, Felipe José Alves de Albuquerque¹, Ruskin Marinho Freitas³

¹UGEO/ITEP, Recife-PE, Brasil, anamonica@itep.br, romilson@itep.br, Correspondence autor.

²UAG/UFRPE, Garanhuns-PE, Brasil, veronicameira@gmail.com

³UFPE, Recife-PE, Brasil, ruskin@ufpe.br

Received in January, 31, 2014; revised in February, 10, 2014; accepted February, 15, 2014.

ABSTRACT

Remote sensing is an indispensable tool in the identification of heat islands in cities, it provides qualitative temperature of the place. Thus, the objective of this study was to estimate and analyze the soil surface temperature for the city of Recife, highlighting the neighborhoods of Good Voyage and Lowland, through satellite image LANDSAT 5-TM, to contribute to the identification of heat islands in urban centers from remote sensing techniques from the model SEBAL - Surface Energy Balance for Land Algorithm developed Bastiaanssen Win in 1998. The results showed that the use of remote sensing for estimating soil temperature appeared as an indispensable tool for identification and interpretation of heat islands in the city of Recife, where heat islands were diagnosed in some neighborhoods of Recife, with emphasis Good for travel that had temperatures up to 35oC. With this study, managers can use the tool to identify heat islands, and able to perform better planning, aiming thermal comfort and consequently improve the quality of life in urban centers.

Keywords: Remote sensing, LANDSAT 5-TM, temperature.

Introduction

The Urban Heat Island phenomenon is a consequence of the occupation and development of large cities process. Amounts of hot air are present in higher concentration in the center of cities, whose populations suffer from this imbalance. And this condition hinders evaporation, reduces the power of dispersion of air pollutants generated by bringing environmental imbalances (Weng et al , 2004).

Remote sensing has been used in urban areas to assess the phenomenon of "urban heat

island" , to perform classification of land use and also to provide input data for models of atmospheric changes and urban area (Voogt & Oke , 2003) . This technology is used in urban centers, as they are great modifiers climate and the scarcity of information, mainly observed in developing countries like Brazil, leading researchers to develop and set models where the input data can be obtained through the use of remote sensing.

A considerable interest has been shown in recent years on the study of urban

climatology, due to the influence of climate on the environment. It is necessary to meet local and regional climatic variations to guide urban planning and selection of the most suitable sites for construction of buildings, materials to be used, among others. Significant increases in temperature are found in climate records of many cities worldwide, mainly related to urban growth and the replacement of green areas by buildings, asphalt, among others.

Kukla et al. (1986) showed that the warming trend observed in recent years, modifying the mean surface global and hemispheric scale temperature can be related to urban growth, since the effects of urban heat island produce a large variation in temperature, similar to that associated with the increase of greenhouse gases in the atmosphere.

Remote sensing, understood as "a form of information of an object or target without any physical contact with the same" (ROSA, 2001, p.1), has emerged as an effective technique for research in geoenvironmental studies by subsidizing the acquisition of a range of data from any location of the globe with temporal records listed (the example, the immense availability of images of CBERS and Landsat images in the catalog of the National Institute for Space Research - INPE), making possible studies in different scales, plus the ability to monitor an area or phenomenon.

Due to the absence of a network of weather stations which can provide data relatively extensive areas associated with great difficulty accessing the data of air temperature, remote sensing spent primarily from the 1970s, to be quite employed to identify and analysis of the phenomenon of heat islands, if possible, [...

] beyond the visions at different scales, perform measurements through the thermal infrared sensor data in apparent surface temperature (land surface temperature - LST), providing qualitative temperature town, or the design of local temperature (COLTRI et al., 2007, p . 5151) .

Currently one of the ways to obtain the surface temperature is through pictures sensors aboard satellites, as well as favoring views of different scales and time, allows the processing of data in the thermal infrared apparent surface temperatures. The temperature quantified by satellite is the radiant surface temperature which is a value higher than the air temperature (WENG 2004).

Lima et al. (2001) say that due continental dimensions of Brazil the remote sensing is an indispensable tool for understanding and monitoring of natural resources.

In this sense, it is increasingly common use of the thermal band for climate studies whose "main characteristic sensitivity to phenomena related to thermal contrasts, serving to detect thermal properties of rocks, soils, vegetation and water" (http://www.dgi.inpe.br/Suporte/files/Cameras-LANDSAT57_PT.php , accessed 15/07/2012) . In Brazil the main satellites are used Landsat 5 - TM , which has a sensor with 120 meters spatial resolution and NOAA (National Oceanic & Atmospheric Administration) board that carries the AVHRR (Advanced Very High Resolution Radiometer) with a spatial resolution of 1km . Several authors have used these data to study the surface temperature, its causes and consequences : Using the thermal band to raising

temperature values an initial discussion of orbital data for the identification of heat islands Birth (2009) , Evolution of urban growth Blumenau (Santa Catarina) and its relation with the increase of the thermal field with data from TM / Landsat 5 (Lima et al., 2009) .

Thus, the objective of this work is to estimate and analyze the temperature of the soil surface to the city of Recife, especially the districts of Boa Viagem and Lowland, through image - LANDSAT 5 TM, to contribute to identifying the heat islands in urban centers from remote sensing techniques.

Characteristics of the study area

The city of Recife occupies a central position on the coast of northeastern Brazil, reaching 800 km from the regional cities of Salvador and Fortaleza. The tropical - humid climate and natural environments composed of beaches, rivers, wetlands, forests and springs are a unique richness and attaches to Recife features that differentiates it from other cities in Brazil. The average annual rainfall is 2,305 mm, with the wettest four months from April to July, and the driest October-December quarter. In this period, we highlight the months of June (390 mm) and July (357 mm) and the wettest November (38 mm) and December (56 mm) the driest (Souza et al , 2012). The average annual relative humidity of the air is around 80 %, with the minimum maximum value in November (74 %) and June (86 %). The climatology of maximum annual air temperature is 29.3 C and minimum of 22.1 ° C, with the months of January and February with the highest values of 30.4 C and 30.5 C , respectively , while July (27.5 C) and August (27.7 ° C) are

the months with the lowest values observed . With respect to minimum temperatures , during the months of February and March the highest minimum amount to 22.9 o C , and in August (20.7 ° C) and July (21.0 ° C) records the lowest (SOUZA, 2011) .

The urbanization of the city took from the Bairro do Recife, with the rapid growth in the nineteenth century. In this period , the city already pointed to its current urban structure , radiocêntrica , star-shaped and in five directions (north , south , east , west and northwest) , resulting from the connection between their original core and old mills . While it grew, the city moved toward the suburbs. The city of Recife is formed by Hills (67.43 %) , Plains (23.26%) and Water areas (9.31 %) , highlighting the areas within these Special Areas of Environmental Conservation - ZEPA (5.58 %) and the long beach of 8.6 km , with 94 districts as shown in Figure 1 (Prefeitura do Recife, 2008).

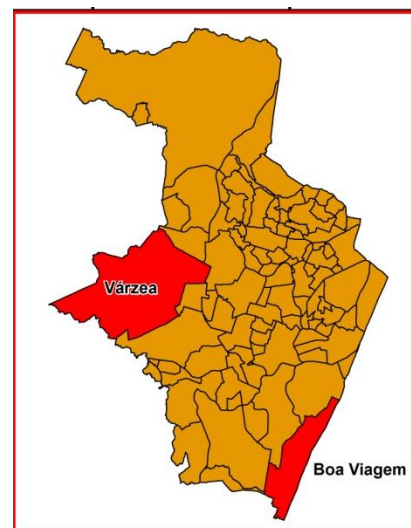


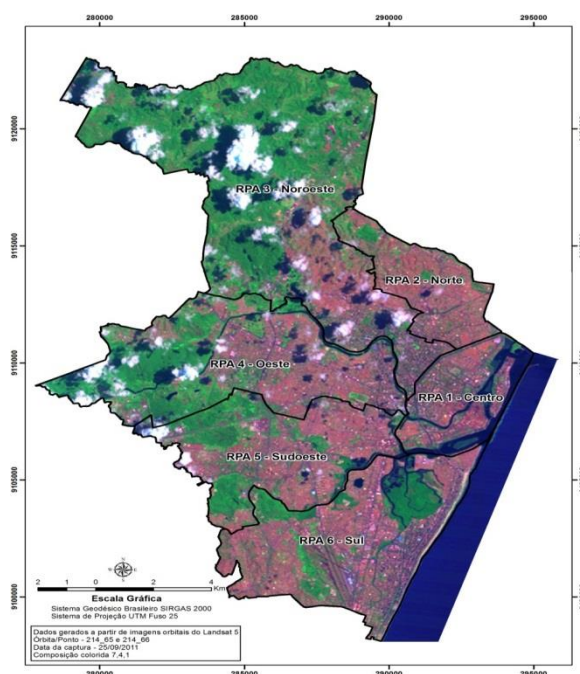
Figure 1 – Recife localization, the red area is Boa Viagem and Varzea.

For this research we selected two distinct neighborhoods in the city of Recife Boa Viagem (South Zone) and Lowland (North Zone). The Boa Viagem district was chosen because it has

the largest population of Recife with 122,922 inhabitants (IBGE, 2010). The neighborhood Lowland vegetation to present the largest city, and is considered the third most populous borough with 70,453 inhabitants (IBGE, 2010).

MATERIALS AND METHODS

TM, orbit 214, paragraph 65 and 66, the date of the scene - to estimate and analyze the surface temperature in the districts of Boa Viagem and Floodplain located in the city of Recife, the thermal infrared images (channel 6) Landsat 5 were used 25/09/2011 with 120 meters spatial resolution, resampled to 30 meters, Julian day: 268, Angle of Elevation: 60.4358 cosine of the Zenith Angle: 0.86980338 (Figure 2) obtained without charge through the website www.dgi.inpe.br.



Figur2 2. Landsat 5 – TM image, 25/09/2011 data. Source: www.dgi.inpe.br

Initial research was conducted for selection of site www.dgi.inpe.br two scenes (214_65 and 214_66) that make up the city of Recife. The criterion for selection of the images was cloud cover. The period chosen was imaging the month of September 2011, a period which has little cloudiness, to be part of the driest quarter of the city of Recife, with average rainfall of 113 mm and an average temperature of 22.4 oC (SOUZA, 2011) .

After selection, the downloads were made for each spectral band and stacking the same, transforming scenes color composite (RGB) . Completed this process , the scenes were mosaicked and geometrically corrected with reference to a picture of orthorectified satellite from checkpoints collected without field. Finally , the cutout (subset) of the mosaic to the limit of the municipality was conducted . Image processing was performed using the software ERDAS IMAGINE 2011 and the statements prepared by ArcGIS 10 , available at ITEP .

To perform the radiometric calibration Table 1 which shows the description of the bands Thematic Mapper (TM) Landsat 5, with corresponding ranges of wavelength calibration coefficients (minimum - and maximum radiance -b) was used and spectral irradiance at the top of the atmosphere (TOA) as described in steps 1 through 6 below.

Table 1: Description of the bands of Thematic Mapper (TM) Landsat 5, with corresponding ranges of wavelength calibration coefficients (radiance minimum - maximum e - b) and the spectral irradiances at the top of the atmosphere (TOA).

Band	Wavelength (µm)	Calibration Coefficient (Wm ⁻² sr ⁻¹ µm ⁻¹)		Irradiance (Wm ⁻² µm ⁻¹)
		a	b	
Band 1 (blue)	0.45 – 0.52	-1.52	193.0	1957
Band 2 (green)	0.52 – 0.60	-2.84	365.0	1826
Band 3 (red)	0.63 – 0.69	-1.17	264.0	1554
Band 4 (Near-Infrared)	0.76 – 0.79	-1.51	221.0	1036
Band 5 (Medium Infrared)	1.55 – 1.75	-0.37	30.2	215,0

Banda Infrared)	6	(thermal	10.4 – 12.5	1.2378	15.303	-
Banda infrared)	7	(Medium	2.08 – 2.35	-0.15	16.5	80,67

Radiometric Calibration - Step 1

The first step is the computation of the spectral radiance of each band (L_{λ_i}), namely the effective radiometric calibration, wherein the digital number (ND) of each pixel of the image is converted into monochromatic spectral radiance. These represent the radiance reflected solar energy per pixel per unit area, time, solid angle and wavelength, measured Landsat (705 mi) level to bands 1, 2, 3, 4, 5 and 7; 6 band, this radiance is the energy emitted by each pixel, and the calibration is carried out according to the equation (Markham & Baker, 1987):

$$L_{\lambda_i} = a_i + \frac{b_i - a_i}{255} ND$$

where a and b are the minimum and maximum spectral radiance (Table 1); ND is the pixel intensity (digital number- integer from 0 to 255); i corresponds bands (1, 2, ..., 7) Landsat 5 - TM.

Reflectance - Step 2

Step 2 is the monochromatic reflectance computation of each band defined as the ratio of the reflected radiation flux and flux incident radiation which is obtained according to the equation (Allen et al, 2002)

$$\rho_{\lambda_i} = \frac{\pi \cdot L_{\lambda_i}}{k_{\lambda_i} \cdot \cos Z \cdot d_r}$$

where L_{λ_i} is the spectral radiance of each band is the spectral irradiance of each band at the top of the atmosphere, (Table 1), Z is the solar zenith angle and d_r is the square of the ratio between the average Earth-Sun distance (r_0) and the distance Sun-Earth (r) given day of the year (DSA), which according to Iqbal (1983), is given by:

$$d_r = 1 + 0,033 \cos(DSA \cdot 2\pi / 365)$$

where DSA is the sequential day of the year and the argument of the function cos in radians. The average annual value is equal to 1.00 and it varies between 0.97 and 1.03 approximately.

When the study area is small or zero slope, the cosine of the angle of incidence of

Fonte: Chander e Markham (2003).

solar radiation is simply obtained from the angle of elevation of the sun - and that is in the image header, ie:

$$\cos z = \cos\left(\frac{\pi}{2} - E\right)$$

where the argument of cos is in radian.

Planetary Albedo - Step 3

Step 3 represents the computation of the planetary albedo, that is, not adjusted albedo atmospheric transmissivity, which is obtained by linear combination of monochromatic reflectance:

$\alpha_{toa} = 0,293\rho_1 + 0,274\rho_2 + 0,233\rho_3 + 0,157\rho_4 + 0,033\rho_5 + 0,011\rho_7$
where ρ_i are the planetary bands 1, 2, 3, 4, 5 and 7 albedo.

Surface Albedo - Step 4

In Step 4 gives the calculation of surface albedo and albedo corrected for atmospheric effects, by the equation:

$$\alpha = \frac{\alpha_{toa} - \alpha_p}{\tau_{sw}}$$

where the planetary albedo is the solar radiation reflected by the atmosphere which varies between 0.025 and 0.04, but for the SEBAL model is recommended to use the value of 0.03, based on Bastiaanssen (2000) and is the Atmospheric transmissivity than for clear sky conditions, can be obtained by (Allen et al, 2002.)

$$\tau_{sw} = 0,75 + 2 \cdot 10^{-5} z$$

where z is the height of each pixel (M). If the user already has a DEM of your area of interest, it may calculate the transmissivity of each pixel, which is recommended for areas with very steep topography. For the sake of simplicity, we use $z = 376$ m which is the altitude of the city of Petrolina - PE, admitted that in the area of Figure 2 was the same constant for all pixels,

yielding $\tau_{sw} = 0,7575$.

Vegetation indices : NDVI, SAVI and LAI - Step 5

Index Normalized Difference Vegetation (Normalized Difference Vegetation Index - NDVI) is obtained by the ratio between the difference of the IR reflectivity close (ρ_{IV}) and red (ρ_V), the sum of the same:

$$NDVI = \frac{\rho_{IV} - \rho_V}{\rho_{IV} + \rho_V}$$

where and are respectively the bands 4:03 Landsat 5 - TM.

The NDVI is a sensitive indicator of the amount and condition of vegetation . Their values range from -1 to +1 and surfaces with some vegetation NDVI ranges from 0 to 1 , since the water and clouds NDVI is generally less than zero .

For the calculation of Adjusted Vegetation Index for the Effects of Soil (Soil Adjusted Vegetation Index - SAVI) which is an index that seeks to mitigate the effects of the " background " of the soil , the expression (Huete , 1988) was used :

$$SAVI = \frac{(1+L)(\rho_{IV} - \rho_V)}{(L + \rho_{IV} + \rho_V)}$$

where L is constant . In a recent study, we used $L = 0.1$, although its most frequent value is $L = 0.5$ (Huete & Warrick, 1990; Accioly et al , 2002; . Boegh et al , 2002).

The Leaf Area Index (LAI) is defined as the ratio of leaf area of all vegetation per unit area used by this vegetation . The LAI is an indicator of biomass of each pixel of the image and the same was computed by the following empirical equation obtained by Allen et al. (2002)

$$IAF = - \frac{\ln\left(\frac{0,69 - SAVI}{0,59}\right)}{0,91}$$

Emissivities - Step 6

To obtain the surface temperature , the Planck equation inverted, a valid black body is used. As not every pixel emits electromagnetic radiation like a black body, there is a need to introduce the emissivity of each pixel in the spectral domain of the thermal band, which is: 10.4 to 12.5 micrometers. In turn , when the computation of long wave radiation emitted by each pixel, is to be considered the emissivity in

the field of broadband (5-100 mM). According to Allen et al. (2002) , and the emissivity can be obtained, for $NDVI > 0$ and $LAI < 3$ according to :

$$\varepsilon_{NB} = 0,97 + 0,00331IAF$$

$$\varepsilon_0 = 0,95 + 0,011IAF$$

For pixels with . For water bodies ($NDVI < 0$) in the case of Sobradinho and milk São Francisco River , Silva & Candide (2004) used values of 0.99 and 0.985 , according to Allen et al. (2002).

Surface Temperature - Step 7

To obtain the surface temperature () the spectral radiance of thermal emissivity and the band obtained in the previous step are used . Thus , one obtains the surface temperature (K) by the following expression:

$$T_s = \frac{K_2}{\ln\left(\frac{\varepsilon_{NB} K_1}{L_{\lambda,6}} + 1\right)}$$

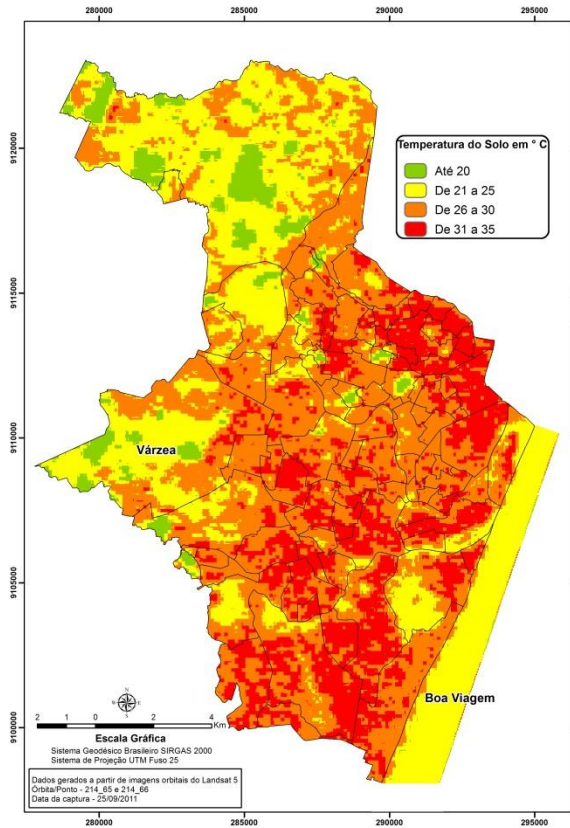
where and are constant calibration of the thermal band of Landsat 5 -T (Allen et al , 2002; . Silva et al , 2005).

Results and Discussion

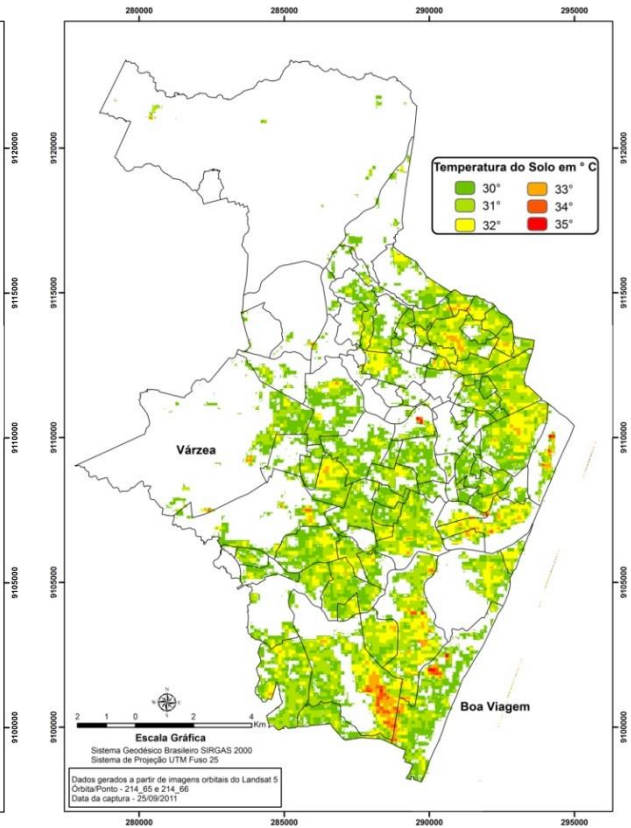
Figure 3 shows the spatial distribution of the temperature of the soil surface obtained from remote sensing techniques (Figures 1a, b and c) and the total population in the districts of Recife (Figure 1d) . In general, the lowest values of the temperatures are observed in the northeast and west of the city of Recife, areas that present the greatest cover crops (Figure 1c), while the highest temperatures in the northern and southern sectors, the most populated regions (Figure 1d). In Figure 1b are identified areas that have higher or equal to 30oC temperatures, especially in the districts of Boa Viagem and Lowland (study area of this work). In Boa Viagem, the temperature of the soil surface is around 30 to 31 oC, highlighting an area with temperatures reaching 35 ° C, showing the formation of a heat island in the region, the mediations of Avenida Domingos Ferreira, whose area there are specific large concrete roofing and intense movement of vehicles which are suitable indicators for the formation of heat islands . On the other hand, in the Lowland district the highest temperatures were observed

in the eastern sector, bordering the neighborhoods of Cured and University City, with temperatures around 30 to 31 oC with identification of only two small nuclei with values around 32 oC, areas covered with

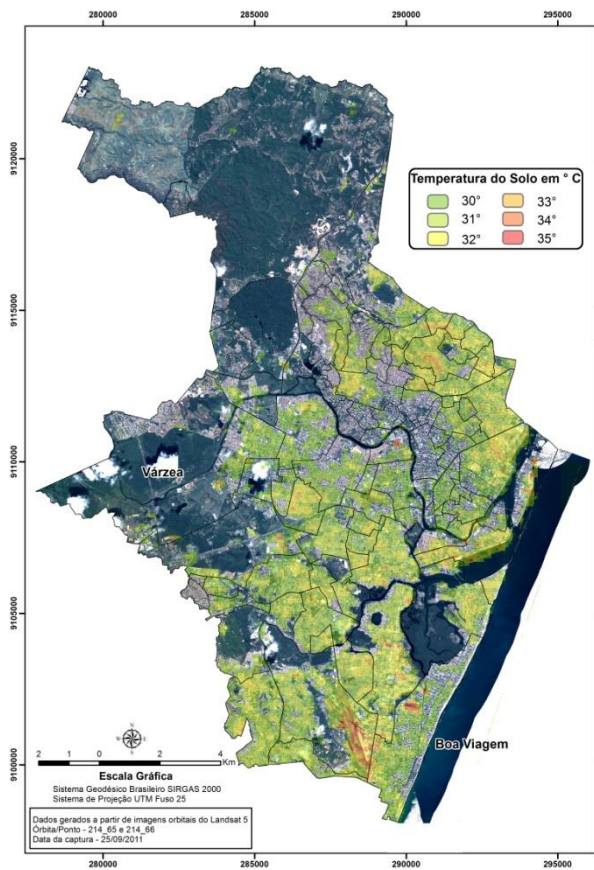
concrete. The temperatures are lower in the Lowland region in relation to the Boa Viagem Neighborhood, due to present the greatest vegetation cover in the city.



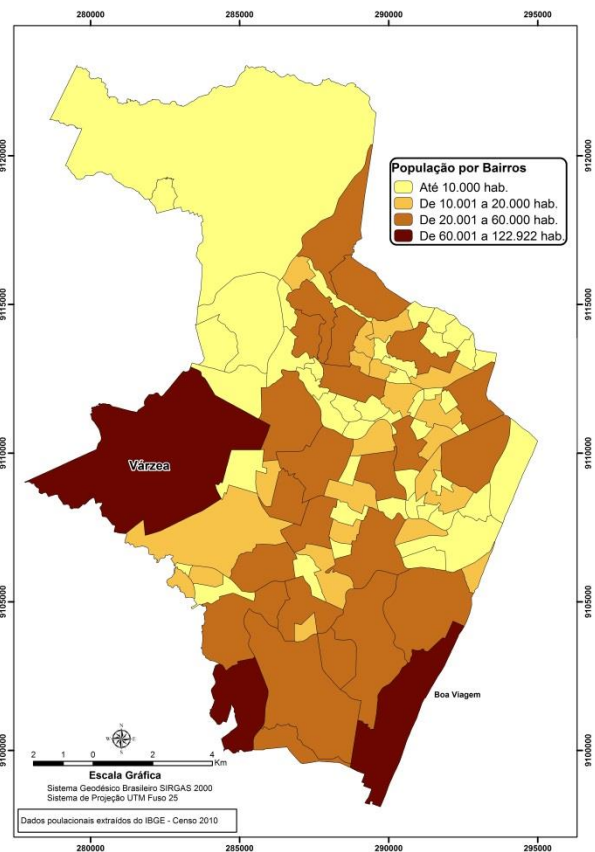
(a)



(b)



(c)



(d)

Figure 3. Spatial distribution of surface temperature (a,b e c) in Recife city and population (d).

Final considerations

The use of remote sensing to estimate soil temperature was presented as a necessary tool for identification and interpretation of heat islands in the city of Recife.

The diagnosis of heat islands in some neighborhoods of Recife, Boa Viagem highlighting that showed temperatures up to 35°C in mediations Pina, Avenida Domingos Ferreira. High temperatures may be associated with heavy vehicle traffic, asphalt, concrete, among others, which significantly influence the urban thermal discomfort.

With this study, managers can use the tool for identification of heat islands, and able to perform better planning, targeting and thermal comfort in Recife city.

Reference

Allen, R.G., Tasumi, M., Trezza, R., Waters, R. & Bastiaanssen, W, 1995. Surface Energy Balance Algorithm for Land – Manual SEBAL.

Atlas do Desenvolvimento Humano do Recife. Prefeitura do Recife. 2002.

Coltri, P. P. et al. 2007. Ilhas de Calor da estação de inverno da área urbana do município de Piracicaba, SP. Simpósio Brasileiro De Sensoriamento Remoto, 13, Florianópolis. Anais do XIII SBSR, Florianópolis, p. 5151–5157.

IBGE. Censo Demográfico 2010. Disponível em <<http://www.ibge.gov.br/home/estatistica/populacao/censo2010>>.

Kukla, G.; Gavin, J.; Karl, T.R. 1986. Urban warming. *Journal of Applied Meteorology*, v.25, p.1265-1270.

Lima, C. O.; Barbosa, M. P.L.; Vera, L. A. S., Miguel, J. 2001. Uso de imagens TM/Landsat-5 e termometria na identificação e mapeamento de solos afetados por seca na região de Sousa, PB. In: *Revista Brasileira de Engenharia Agrícola e Ambiental*, v.5, n.2, p.361-363, Campina Grande, PB, DEAG/UFPB.

Lima, G.S.; Liesenberg, V; Souza, C.M.M. 2009. Evolução do Crescimento urbano em Blumenau (Santa Catarina) e a sua relação com o aumento do Campo Térmico com dados TM/Landsat. In: *Simpósio Brasileiro*

- De Sensoriamento Remoto, 14, Natal. Anais XIV SBSR, Natal/RN, p. 1409-1415.
- Lombardo, M. A. 1996. Ilha de calor nas metrópoles – o exemplo de São Paulo. Editora Hucitec, p.224, São Paulo.
- Monteiro, C. A. F. 1976. São Paulo: IGEOG/USP, (Série Teses e Monografias).
- Nascimento, Diego Tarley Ferreira; Barros, Juliana Ramalho. 2009. Identificação de ilhas de calor por meio de sensoriamento remoto: estudo de caso no município de Goiânia/GO/2001. Boletim Goiano de Geografia, Goiânia, v. 29, p. 119-134.
- Prefeitura Do Recife. 2008. A Cidade do Recife: Perfil e História. Disponível em : < <http://www.recife.pe.gov.br/pr/secplanejamento/inforec/>>; Acesso em 08 de julho.
- Rosa, R. 2001. Introdução ao sensoriamento remoto. 4º ed. Uberlândia: Ed. da Universidade Federal de Uberlândia, 210 p.
- Spronken-Smith, R.A. 1994. Energetics and cooling in urban parkes. Vancouver: Unpubl.Ph.D. Thesis. The University of British Columbia, 204 p.
- Souza, W.M. De, Azevedo, P.V. De E Araújo, L.E De. 2012. Classificação da Precipitação Diária e Impactos Decorrentes dos Desastres Associados às Chuvas na Cidade do Recife-PE. Revista Brasileira de Geografia Física. V(2), pag. 250-268.
- Stulpnagel, A.V.; Hobert, M.; Sukopp, M. 1990. The Importance of vegetation for the climate. Urban Ecology, p. 175-193.
- Voogt, J. A.; Oke, T. R. 2003. Thermal remote sensing of urban climates. Remote Sensing of Environmet. Vol. 86,p. 370-384.
- Weng, Q. Dengsheng, L. Schubring, J. 2004. Estimation of land surface temperature–vegetation abundance relationship for urban heat island studies. Remote Sensing of Environment 89, v.66, n.23,p,467– 483.